Advance Sustainable Science, Engineering and Technology (ASSET)
Vol. 8, No.3, July 2026, pp. 02603026-01 ~ 02603026-011
ISSN: 2715-4211 DOI: https://doi.org/10.26877/asset.v8i3.3591

CFD Simulation of Flame Characteristics Resulting from Volatile Matter Combustion of Various Biomass Pellets

Ramavi Akbar Akhsanul Fitrah[1], Ratna Dewi Kusumaningtyas[1]*, Dwi Widjanarko[2], Catur Rini Widyastuti[1], Muslikhin Hidayat[3], Muhammad Aziz[4]

[1]Chemical Engineering Department, Faculty of Engineering, Universitas Negeri Semarang, Sekaran, Gunung Pati, Semarang, Central Java 50229, Indonesia.

[2]Automotive Engineering Education Department, Faculty of Engineering, Universitas Negeri Semarang, Sekaran, Gunung Pati, Semarang, Central Java 50229, Indonesia.

[3]Department of Chemical Engineering, Faculty of Engineering, Universitas Gadjah Mada, Jl. Grafika No.2, UGM Campus, Yogyakarta, 55281, Indonesia.

[4]Institute of Industrial Science, The University of Tokyo, 4-6-1 Komaba, Meguro-ku, Tokyo 153-8505, Japan

*ratnadewi.kusumaningtyas@mail.unnes.ac.id

Abstract. While biomass is a promising carbon-neutral alternative to coal, the specific volatile matter (VM) flame characteristics of diverse biomass pellets, particularly water hyacinth, remain under-researched. This study uses a numerical CFD approach (Ansys Fluent) to investigate how varying VM fractions influence flame structure in a 2D planar slice of the furnace block (25 cm width). Simulations employed the SST k–ω turbulence and Eddy dissipation model to capture mixing-limited chemical reactions. Boundary conditions were based on experimental configurations using a 0.05 m/s air inlet velocity. Results using CO-based flame-tip markers revealed that water hyacinth (VM: 63.5 wt%) produced a peak temperature of ~1,400°C at 75 cm above the fuel, while rice husk and bagasse (VM: 59–77 wt%) exhibited longer, more intense hot plumes compared to the localized heat profile of coal. These findings demonstrate that biomass generates more dispersed combustion zones, aiding in furnace hot-spot prevention and air control optimization. A limitation of this study is that findings are based solely on numerical simulations without direct experimental validation, although the model replicates physical furnace configurations. These results provide a foundation for developing sustainable biomass–coal co-firing technologies.

Keywords: Biomass pellets, CFD, co-firing, flame length, non-premixed combustion

(Received 2026-03-15, Revised 2026-04-09, Accepted 2026-05-11, Available Online by 2026-06-12)

1. Introduction

Global energy consumption is currently dominated by fossil fuels, such as coal, which are limited in supply and contribute to increased greenhouse gas emissions and air pollution [1]. Therefore, a shift to cleaner, renewable energy sources is urgently needed [2]. Biomass is a promising candidate as an alternative fuel because it is considered carbon neutral, meaning the carbon dioxide (CO_2) released during combustion is generally equivalent to that absorbed by plants during their growth phase. By partially replacing coal with biomass, CO_2 emissions can be reduced, thereby supporting global efforts to mitigate climate change. The use of biomass is also expected to reduce emissions of other pollutants that are major problems associated with coal combustion, such as carbon monoxide (CO), nitrogen oxides (NO_x), sulfur oxides (SO_x), and particulate matter [1], [3-5]. Biomass generally contains lower amounts of nitrogen and sulphur, so its combustion produces significantly less NO_x and SO_x [6-7]. Experimental studies have shown that adding 10–30% biomass to a coal mixture can reduce NO_x emissions by approximately 19–42% and SO_x emissions by approximately 24–39% [8]. Meanwhile, CO emissions from biomass combustion are also influenced by the efficiency of the combustion reaction (because biomass contains oxygen in its chemical structure). The oxidation of CO-to-CO_2 occurs more easily during optimal combustion. Therefore, using biomass as an alternative fuel can significantly reduce harmful pollutants compared to conventional coal combustion.

Indonesia is abundant in various types of biomasses, including water hyacinth (*Eichhornia crassipes*), rice husks, bagasse, and sawdust [9-10]. Each biomass has distinct combustion characteristics compared to coal. Generally, these biomasses have high moisture and volatile matter (VM) content, resulting in lower ignition and burnout temperatures [1], [11-12]. Thermogravimetric studies have shown that biomass samples begin to react at lower temperatures than coal due to their high volatile content [1], [13]. In contrast, sub-bituminous coal typically contains a higher total carbon content and requires higher combustion temperatures for complete oxidation [1], [12], [14]. These differences in properties result in significant variations in the temperature profiles and combustion reaction rates between biomass and coal. Furthermore, the ash content and calorific value of biomass (usually lower) differ from those of sub-bituminous coal, thus affecting the thermal efficiency and combustion residues of these fuels [1], [4], [7], [13]. The optimization of biomass-to-binder ratios is also critical for enhancing combustion efficiency, as demonstrated in studies where specific formulations achieved high calorific values of up to 7,192 kcal/kg while maintaining low ash content (3.57%) [15].

Several recent studies have examined how biomass composition affects flame height and temperature during volatile combustion [16-19]. All of those studies are laboratory-scale and often use idealized fuels (single particles, pellets, or liquids) and burners. They clearly show that higher volatile matter and smaller particle size increase flame height and temperature. However, each setup has restrictions – e.g. pellet binding, instrument measurement limits, or focus on the volatile envelope only. Studying biomass combustion characteristics requires a thorough understanding of the reaction processes and combustion turbulence. Numerical simulations using Computational Fluid Dynamics (CFD) software such as Ansys Fluent (ANSYS Inc.) are instrumental in this regard. CFD methods enable simultaneous modelling of fluid flow, species transport, heat transfer, and chemical reactions within the combustion chamber [20]. Through simulation, researchers can estimate temperature distribution, gas species concentrations (CO, CO_2, NOx, SOx), and fuel mass conversion at various locations within the combustion chamber based on specific chemical reaction models [20-23]. Such simulations help identify heat distribution and emission patterns, as well as examine the influence of design parameters and operating conditions (e.g., air flow rate or furnace geometry) on combustion performance. Therefore, the CFD approach enables the optimization of the combustion system to enhance co-firing stability, hot-spot prevention, and furnace operational control.

Despite the established understanding that higher volatile content generally leads to taller flames, there is a significant data gap regarding the localized thermal profiles and flame-tip trajectories of invasive aquatic biomass, such as water hyacinth, when processed into pellets. Furthermore, a consistent

comparison of these characteristics against traditional biomass and coal under identical furnace boundary conditions is lacking. Moving beyond established correlations between volatile content and flame height, this study uncovers a non-linear relationship driven by the competing thermal ballast effects of moisture and ash specifically in water hyacinth and other local biomasses. This allows for a more nuanced 'energy-density ratio' approach to furnace air-control that cannot be achieved through proximate analysis alone. The primary novelty lies in the application of a CO-based flame-tip definition to quantify the combustion behavior of water hyacinth pellets. The contributions of this work include: (i) a quantified comparison of flame heights across five biomass types and coal, (ii) the identification of peak temperature zones relative to VM fraction, and (iii) technical insights into air-velocity control for optimizing biomass co-firing in industrial furnaces.

2. Methods

The CFD software used in this study is Ansys Fluent version 2025 R2. This program can be utilized to specify custom sub-models with biomass input in the combustion process. Reynolds-averaged Navier-Stokes (RANS) conservation equations are solved for the continuous phase in the Eulerian reference frame. Second-order upwind algorithms are used to solve the continuity equations, momentum, energy balance, and component transport balance in the presence of chemical reactions. The Shear-Stress Transport (SST) k–ω turbulence model is applied to this configuration because it can represent the swirling flow behavior. The SST k–ω turbulence model was paired with the Eddy Dissipation Model (EDM) to specifically address the mixing-limited nature of the turbulent volatile flame. While EDM simplifies the reaction kinetics into a two-stage process, it is highly effective for identifying the global flame structure and peak temperature zones in industrial-scale simulations where turbulence dominates finite-rate chemistry [24]. The constants A (applied to the reactant species) and B (applied to the product species) in the turbulent mixing rate equations used in this simulation are 4.0 and 0.5, respectively [25]. The discrete ordinate radiation model is applied to solve the radiative transport equation. The computational domain is a two-dimensional (2D) computational grid with 1,853 rectangular grid elements. The dimensions of the simulated burner furnace represent a 2D planar slice of the furnace block with a width of 25 cm with a domain height of 1.15 m equipped with an air fan with dimensions of 10 cm × 10 cm and a biomass pellet particle insertion place with a slope of 3:2. This non-axisymmetric approach was selected to focus on the cross-sectional flame development and species transport along the primary flow path. While this assumes a degree of uniformity across the furnace width, it allows for a more detailed observation of the longitudinal VM plume and hot-spot distribution within a simplified computational framework.

To ensure that the numerical results were independent of the computational grid, a tri-level (Coarse (1,853 elements), Medium (4,173 elements), and Fine (9,462 elements)) mesh refinement study was conducted, employing metrics such as the Convergence Ratio to verify monotonic convergence within the asymptotic range [26]. Evaluation of the longitudinal CO mass fraction and temperature profiles indicated that the Coarse mesh effectively captured the primary flame structure and peak temperature gradients with high stability. Given the comparative nature of this study (which focuses on the relative differences between multiple biomass types rather than absolute experimental replication), the Coarse mesh was selected to maintain a robust balance between numerical convergence and computational economy. To ensure numerical credibility in the absence of direct experimental validation, a rigorous grid-independence test was performed. Results from the Medium and Fine meshes showed less than a 10% difference in peak temperature & peak location compared to the Coarse mesh, confirming that the primary flame structure is effectively captured. This methodology follows established practices for comparative CFD studies where the focus is on identifying trends between fuel variations under identical boundary conditions.

Boundary conditions were specified based on process data and equipment configuration during the experiment. Air injection was specified with an inlet velocity of 0.05 m/s, a temperature of 27 °C, and an oxygen (O_2) content of 23% by weight with the balance being nitrogen (N_2) gas. Inlet turbulence

intensity and quantities was defined as 5% turbulent intensity with viscosity ratio of 10. To simulate the reactant in the form of VM, the author deliberately created boundary conditions in the form of walls with 13 spherical (/2D circular) biomass pellet particles with a diameter of 1 cm. On each biomass pellet wall, the boundary conditions were in the form of a mass fraction derived from the VM composition from the proximate analysis and also in the form of thermal conditions in the form of the heat production rate from the combustion reaction. The gas exhaust was set as the pressure outlet boundary condition, with ambient pressure of 1 atm at room temperature with no backflow. The Eddy dissipation model requires reaction product values to initiate the combustion reaction [27]. Therefore, for the ignition process in the steady-state simulation, the mass fractions of all chemical species (VMs, O_2, CO_2, H_2O, CO, and SO_2) were initially set to 0.01, which is sufficient to ignite the combustion reaction. A species mass fraction of 0.01 was used as a numerical seed for initialization as recommended in the Ansys Fluent Documentation [27].

2.1. Biomass Sub-Models

The combustion reaction mechanism was modeled as a two-stage reaction involving SO_2 with the CO/CO_2 split in reaction-1 (Equation 1) being 1, indicating that the molar fraction of CO to CO_2 in reaction-1 consumes all the carbon in the biomass to form CO with no CO_2 produced. Therefore, the reaction equations can be written as Equations 1 and 2 below with stoichiometric coefficients calculated from the proximate and ultimate analyses of each biomass. The VM composition in Equation 1 (vol) is estimated to be 1 long-chain hydrocarbon species based on proximate and ultimate analyses [27]. For reaction equation 1, the kinetic data are in the form of a pre-exponential factor value of 2.12×10^{11} s^{-1}, an activation energy of 2.03×10^8 J/kmol, and a reaction order of $[vol][O_2]$ [27]. Meanwhile, for reaction equation 2, the kinetic data are in the form of a pre-exponential factor value of 2.24×10^{12} s^{-1}, an activation energy of 1.70×10^8 J/kmol, and a reaction order of $[CO][O_2]^{0.25}$ [27]. The results of the proximate and ultimate analyses, as well as the physical and chemical properties of the coal and water hyacinth were taken from our previous studies, where several other biomasses (rice husks [28], sugarcane bagasse [29], ironwood sawdust [28], and teak sawdust [28], [30]) are included as variations/comparative values.

$$vol + v_{O_2}O_2 \rightarrow v_{CO}CO + v_{CO_2}CO_2 + v_{H_2O}H_2O + v_{SO_2}SO_2 + v_{N_2}N_2 \quad (1)$$

$$CO + 0.5O_2 \rightarrow CO_2 \quad (2)$$

2.2. Definition of The Flame Tip of VMs

In non-premixed fuel gas combustion flames, CO, CO_2, and O_2 concentrations have been widely used as markers of the end/tip of the flame [31]. The end/tip of the flame is indicated by the decreasing CO concentration, followed by an increase in O_2 concentration. In this study, we replicated a similar approach to determine the location of the volatile flame. The CO concentration is high on the fuel-rich side of the flame but decreases steadily toward zero outside the flame because oxygen (O_2) is abundant in the outer flame, converting CO to CO_2. The tip of the flame can be identified as the location where the CO concentration decreases rapidly toward zero/or approaches a certain constant value asymptotically close to zero. A commonly used parameter is the CO fraction (Equation 3) [21].

$$CO\ fraction = \left(\frac{[CO]}{[vol]+[O_2]+[CO_2]+[H_2O]+[CO]+[SO_2]+[N_2]}\right) \quad (3)$$

3. Results and Discussion

3.1. Flame Length from Burning Water Hyacinth Pellets (and Other Biomasses)

Table 1 tabulated the summary of flame tip height (based on CO-marker), peak temperature, & qualitative plume width of sub-bituminous coal and five biomasses. The credibility validation of the interpreted flame structures was compared against the semi-empirical correlations for laminar/turbulent jet flames established by Roper [31]. From Figure 1, The transition of the CO-concentration profile and

the subsequent temperature decay in the simulation follow the classical diffusion flame characteristics. Furthermore, the peak temperature recorded for water hyacinth (~1,400°C) aligns with experimental observations of high-volatile biomass pellets in similar small-scale furnace environments [16-17], [19], where peak temperatures typically range between 1,200-1,500°C depending on the excess air ratio.

Table 1. Summary of flame tip height (based on CO-marker), peak temperature, & qualitative plume width of sub-bituminous coal and five biomasses

Materials	Flame tip Height (m)	Peak Temperature (^{o}C)	Plume Width
Coal	0.18	1159	shorter plumes and lower, more concentrated maximum temperatures
Water Hyacinth	0.75	1438	intermediate pattern; diffused hot peaks
Rice Husks	0.87	1481	longer hot columns and higher peak temperatures
Sugarcane Bagasse	1.10	1572	longest hot columns and highest peak temperatures
Ironwood Sawdust	0.78	1412	intermediate pattern; diffused hot peaks
Teak Sawdust	0.74	1209	intermediate pattern; diffused hot peaks

The determination of flame tip height is exemplified in Figure 1. The peak (Figure 1, blue line) at x ~15 cm is located in the fuel-rich flame zone, where intense volatile release occurs and minimal oxygen is present. The peak in Figure 1 is preceded by reaction 1 (orange line) which is then followed by a CO peak (blue line) which forms two bumps (or "bimodal"). At the reaction peak, volatiles mix and react with oxygen to produce CO gas which is then turbulently propelled to form the first bump of the CO curve. After that, the rate of reaction 1 immediately decreased until it disappeared due to the non-stoichiometric occurrence of the combustion reaction. After a significant amount of CO was formed, they were ready to react with oxygen according to Reaction Equation 2. The CO fraction reached its minimum values at a height of 75 cm or about 60 cm from the disappearance of combustion reaction 1. This is the CO exhaustion (i.e. tip of the volatile matter flame).

From the sensitivity of the VM released (not shown here) for the combustion at various weight fraction with respect to the flame tip height and peak temperature at constant airflow velocity 0.05 m/s, it can be inferred that the release of volatile matter is influenced by several factors, including volatility, VM content, moisture content, and particle size, which play a significant role in creating the flame shape [21], [32-33]. The sub-bituminous coal sample gives the lowest VM release profile (Figure 2). For biomass-based fuels, the devolatilization process differs from that of coal because the volatile release rate is higher and the onset temperatures are lower than for coal [33], [34]. The magnitude /number of volatiles released from various biomasses, as shown in Figure 2, does not correlate with the VM content, indicating that the values are not correlated. This is because the chemical reaction rates for the reactions of the starting materials, volatiles, with oxygen are usually faster than the rate of mixing due to turbulence for the fuel and oxidizing agent [24]. Consequently, in determining the flame length, the influence of VM composition is less important than the volatile release rate and mixing rate. It has been clarified that while VM provides the 'fuel' for the flame, the flame height is not a linear function of VM percentage alone. For instance, in the case of water hyacinth, the high moisture content 9.9 wt% acts as a thermal ballast, reducing the adiabatic flame temperature and volatile release rate, which explains the shorter flame despite high VM, as compared to rice husk. Also, high ash (like in rice husk) can act as a thermal sink or a physical barrier, slowing down the diffusion of volatiles into the oxidizing environment. Additionally, even if VM wt% is high, a less dense pellet provides less "fuel mass" per unit volume of the reaction zone, leading to a thinner, less persistent flame.

The observed discrepancy between VM content and flame height, where bagasse (higher VM) and water hyacinth (lower VM) display distinct morphology, supports the conclusion that flame structure is determined by the energy-density ratio. In water hyacinth, the specific volatile release rate is tempered by the 9.9 wt% moisture content, which requires significant latent heat for phase change. This effectively 'starves' the early ignition zone of thermal energy, leading to a more elevated peak temperature zone (0.75 m) compared to coal (0.18 m).

3.2. CO_2 Profile and Combustion Temperature of Water Hyacinth Pellets (and Other Biomasses)

Figure 3 shows the numerical profiles of CO_2 mass fraction (blue line, left scale) and temperature (orange line, right scale) along the centerline of the burner height for water hyacinth biomass pellets. The temperature pattern follows a similar trend with the CO_2 fraction: a brief dip near the bottom, then a rise towards a peak at approximately 0.3–0.4 m (peak temperature ~1,400°C) and a slow decline upward. The correspondence between the temperature and CO_2 peaks indicates an active combustion zone in the middle region, producing oxidation products. The decrease in both quantities towards the top of the burner is due to cooling and dilution of the gas stream by the unreacted fan airflow. Overall, this plot illustrates that bio-pellet combustion is focused in the center zone of the furnace, with maximum CO_2 production and heat output at that position, then decreasing as the gas flow rises to the top.

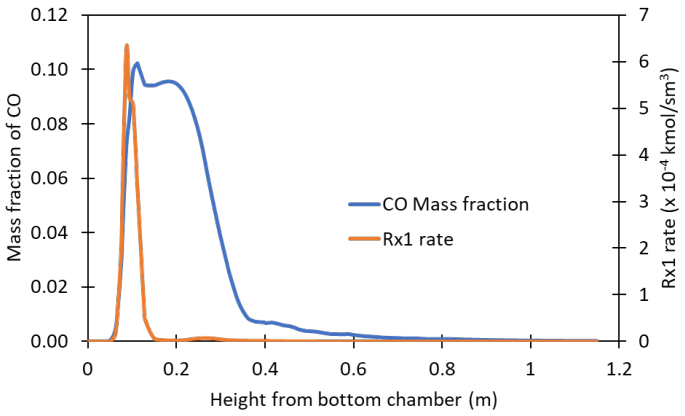

Figure 1. Numerical profiles of CO mass fraction and volatile reaction rate with oxygen along the centreline of the burner height for water hyacinth biomass pellets

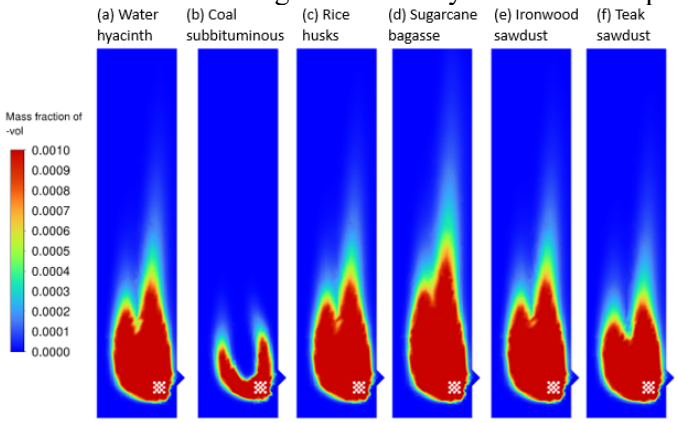

Figure 2. Volatile mass fraction profiles for the combustion of (a) water hyacinth, (b) coal, (c) rice husks, (d) sugarcane bagasse, (e) ironwood sawdust, and (f) teak sawdust.

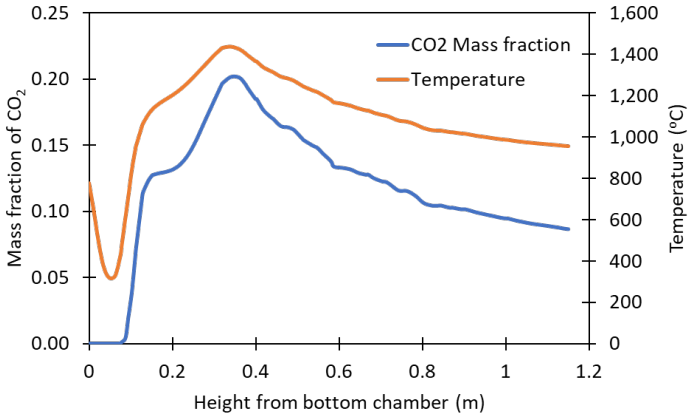

Figure 3. Numerical profiles of CO_2 mass fraction and temperature along the centerline of the burner height for water hyacinth biomass pellets

In all numerical temperature profiles for the combustion of various biomass fuels (not shown here), a hot plume structure is observed rising from the combustion area near the bottom, with the highest temperatures (red/yellow on the scale) concentrated in the core of the gas stream above the fuel surface, while the furnace walls and corners remain relatively cool (blue). Differences between biomass materials are clear: subbituminous coal produces shorter plumes and lower, more concentrated maximum temperatures, while rice husks and sugarcane bagasse display longer hot columns and higher peak temperatures, indicating more intense heat and volatile release; water hyacinth (a biomass with a medium VM of 63.47 wt.%) and both types of sawdust (ironwood and teak, biomass with a high VM of >71 wt.%) show an intermediate pattern with somewhat diffused hot peaks. These vertical and lateral temperature gradients reflect the differences in combustion characteristics of each material (e.g., volatile composition and reaction rate) and are important for burner design, emission control, and combustion efficiency, as the location and intensity of the combustion zone significantly impact mass conversion, gas temperature, and pollutant formation.

3.3. Insights for Optimizing Combustion of Biomasses in Furnace (using Air-Velocity Control)

Analysis of the flame profiles reveals a nuanced relationship between fuel composition and flame morphology. While a higher VM fraction typically suggests an elongated flame [35], our results show a non-linear correlation. This is primarily attributed to the competing effects of moisture and ash. For example, water hyacinth pellets, despite having a significant VM fraction (63.5 wt%), exhibit a peak temperature zone at ~0.75 m. The presence of moisture (9.9 wt%) requires significant latent heat for vaporization, which locally cools the flame base and slows the kinetic rate of volatile oxidation. Furthermore, the high ash content in rice husk (21.4 wt%) compared to coal (17.6 wt%) serves as a thermal buffer, resulting in a more dispersed and less 'pointed' flame tip. These interactions suggest that furnace air-control must be tuned not just to VM content, but to the energy-density ratio of the specific biomass pellet.

To provide grounded technical insights into air-furnace operation, we performed a parametric study varying the air inlet velocity as presented in Figure 4. When air velocity increases from 0.03 to 0.07 m/s and the flame height drops (blue bars), it indicates that the combustion process transitions from being diffusion-limited to being more mixing-efficient. This inverse relationship is attributed to the enhanced air-fuel mixing rate; higher inlet momentum increases the shear forces between the air stream and the volatile plume, accelerating the oxidation of CO and other intermediate species. Consequently, the volatile matter is consumed closer to the burner base, resulting in a more concentrated heat release zone. This is further supported by the orange curve (peak temperature), which shows that temperature

increases, indicating that while the flame is shorter, it maintains high thermal intensity due to improved combustion efficiency.

Our results show that higher air velocities (0.07 m/s) effectively reduce the flame height of high-VM biomass pellets. This suggests that for biomass fuels like water hyacinth, which naturally produce elongated plumes, increasing secondary air velocity is an effective strategy for preventing flame impingement on upper furnace structures. We have linked this to the mixing-limited nature of the Eddy Dissipation Model used in our study, where increased velocity directly correlates to a faster reaction rate per unit volume, shortening the flame.

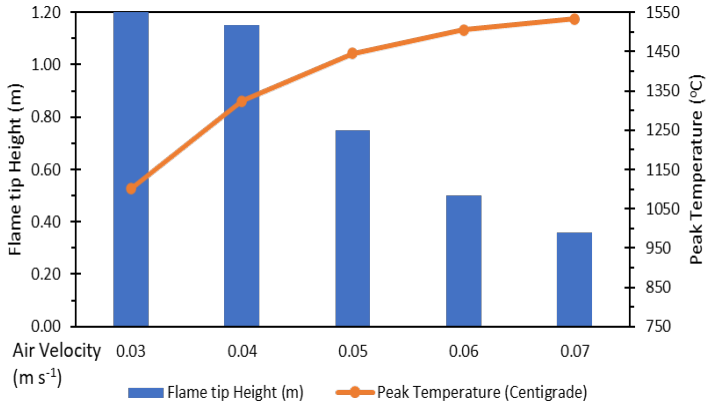

Figure 4. Sensitivity of the airflow inlet velocity for the combustion of water hyacinth with respect to the flame tip height and peak temperature

4. Conclusions

This study demonstrates that the combustion of biomass (water hyacinth, rice husk, bagasse, and sawdust) exhibits distinct characteristics compared to sub-bituminous coal, particularly in terms of volatile matter release, temperature distribution, and reaction rate. Analysis of the flame profiles reveals a nuanced relationship between fuel composition and flame morphology. While a higher VM fraction typically suggests an elongated flame, our results show a non-linear correlation. This is primarily attributed to the competing effects of moisture and ash. The results of CFD numerical simulations with Ansys Fluent indicate that biomass generally releases volatile matter at lower temperatures and with higher intensity than coal, resulting in a wider, more turbulent, and more spread combustion zone towards the top of the furnace. In contrast, coal tends to produce more localized combustion with a narrower heat release.

Furthermore, the observed reduction in flame height with increased air velocity explains the lack of a simple correlation between VM wt% and flame length. A fuel with high VM (like Bagasse) may produce a shorter flame than a lower-VM fuel if the local air velocity provides more efficient mixing. Thus, flame morphology is a product of both fuel chemistry (VM content) and burner aerodynamics (air velocity). Our study demonstrates that flame length cannot be predicted by proximate analysis alone but must be evaluated within the context of the furnace's velocity field.

While this study provides valuable comparative insights into the flame behavior of diverse biomass pellets, several limitations are acknowledged which offer opportunities for future research. For example, the volatile matter combustion was modeled using a two-stage reaction of Eddy Dissipation Model. Future studies could incorporate multi-step kinetics or Flamelet models to better capture intermediate species and finite-rate chemistry effects. For the analysis parts, this study focused on steady-state flame morphology. However, biomass combustion is inherently transient due to the stages of moisture evaporation and char oxidation. Future work should involve transient simulations to capture these time-dependent fluctuations. Also, the findings are currently based solely on numerical simulations. Future investigations will prioritize the collection of experimental flame-imaging data (such as OH-PLIF or high-speed photography) to validate the predicted flame-tip heights and temperature gradients.

Declaration of AI and AI assisted technologies in the writing process

During the preparation of this work the author(s) used Gemini in order to improve the grammatically checking for the manuscript. After using this tool/service, the author(s) reviewed and edited the content as needed and take(s) full responsibility for the content of the publication.

Declaration of Competing Interest

The authors declare that they have no known competing financial interests or personal relationships that could have appeared to influence the work reported in this paper.

Acknowledgements

The authors gratefully acknowledge support from the Research and Community Service Institute (LPPM) of Universitas Negeri Semarang for the financial support through the international collaboration (Top 100) research funding with the contract number of 280.14.3/UN37/PPK.11/2025.

References

[1] Y. Yuan, Y. He, J. Tan, Y. Wang, S. Kumar, and Z. Wang, "Co-Combustion Characteristics of Typical Biomass and Coal Blends by Thermogravimetric Analysis," *Front. Energy Res.*, vol. 9, p. 753622, Oct. 2021, DOI: 10.3389/fenrg.2021.753622

[2] Bayu Triwibowo *et al.*, "Sensitivity Analysis of Bioethanol Simulation from Microalgae with Pressure Swing Distillation Process," *J. Adv. Res. Fluid Mech. Therm. Sci.*, vol. 94, no. 1, pp. 96–107, Apr. 2022, DOI: 10.37934/arfmts.94.1.96107

[3] Y. Jiang, T. Mori, H. Naganuma, and Y. Ninomiya, "Effect of the optimal combination of bituminous coal with high biomass content on particulate matter (PM) emissions during co-firing," *Fuel*, vol. 316, p. 123244, May 2022, DOI: 10.1016/j.fuel.2022.123244

[4] X. Zhang, K. Li, C. Zhang, and A. Wang, "Performance analysis of biomass gasification coupled with a coal-fired boiler system at various loads," *Waste Manag.*, vol. 105, pp. 84–91, Mar. 2020, DOI: 10.1016/j.wasman.2020.01.039

[5] W. Yang, D. Pudasainee, R. Gupta, W. Li, B. Wang, and L. Sun, "An overview of inorganic particulate matter emission from coal/biomass/MSW combustion: Sampling and measurement, formation, distribution, inorganic composition and influencing factors," *Fuel Process. Technol.*, vol. 213, p. 106657, Mar. 2021, DOI: 10.1016/j.fuproc.2020.106657

[6] L. Xu, G. Zhu, and Y. Niu, "Effect of preheating Co-firing of biomass and coal on the synergistic reduction of PM and NO source emissions," *J. Clean. Prod.*, vol. 414, p. 137562, Aug. 2023, DOI: 10.1016/j.jclepro.2023.137562

[7] L. Liu *et al.*, "Recent advances of research in coal and biomass co-firing for electricity and heat generation," *Circ. Econ.*, vol. 2, no. 4, p. 100063, Dec. 2023, DOI: 10.1016/j.cec.2023.100063

[8] A. Zhuikov, D. Glushkov, A. Pleshko, I. Grishina, and S. Chicherin, "Co-Combustion of Coal and Biomass: Heating Surface Slagging and Flue Gases," *Fire*, vol. 8, no. 3, p. 106, Mar. 2025, DOI: 10.3390/fire8030106

[9] Erdiwansyah *et al.*, "Prospects for renewable energy sources from biomass waste in Indonesia," *Case Stud. Chem. Environ. Eng.*, vol. 10, p. 100880, Dec. 2024, DOI: 10.1016/j.cscee.2024.100880

[10] H. Prasetiawan, D. S. Fardhyanti, E. F. C. Purnomo, W. Kusumoayu, and R. A. A. Fitrah, "The Effect of Raw Material Composition and Pyrolysis Temperature on The Characteristics of Bio-Oil from the Pyrolysis of Sawdust and Sugar Cane Bagasse Mixture," *E3S Web Conf.*, vol. 648, p. 03007, 2025, DOI: 10.1051/e3sconf/202564803007

[11] T. Wang *et al.*, "Co-combustion behavior of dyeing sludge and rice husk by using TG-MS: Thermal conversion, gas evolution, and kinetic analyses," *Bioresour. Technol.*, vol. 311, p. 123527, Sep. 2020, DOI: 10.1016/j.biortech.2020.123527

[12] K. Konwar *et al.*, "Effect of biomass addition on the devolatilization kinetics, mechanisms and thermodynamics of a northeast Indian low rank sub-bituminous coal," *Fuel*, vol. 256, p. 115926, Nov. 2019, DOI: 10.1016/j.fuel.2019.115926

[13] S. G. Sahu, N. Chakraborty, and P. Sarkar, "Coal–biomass co-combustion: An overview," *Renew. Sustain. Energy Rev.*, vol. 39, pp. 575–586, Nov. 2014, DOI: 10.1016/j.rser.2014.07.106
[14] S. Munir, S. S. Daood, W. Nimmo, A. M. Cunliffe, and B. M. Gibbs, "Thermal analysis and devolatilization kinetics of cotton stalk, sugar cane bagasse and shea meal under nitrogen and air atmospheres," *Bioresour. Technol.*, vol. 100, no. 3, pp. 1413–1418, Feb. 2009, DOI: 10.1016/j.biortech.2008.07.065
[15] A. P. Heriyanti *et al.*, "Exploring Biochar Briquettes from Biomass Waste for Sustainable Energy," *Adv. Sustain. Sci. Eng. Technol.*, vol. 7, no. 3, p. 0250303, Aug. 2025, DOI: 10.26877/asset.v7i3.1311
[16] L. Yuliati, N. Hamidi, and R. E. Pragiwaka, "Combustion Characteristics of A Wood Pellet Made of Albizia Chinensis and Rice Husk," *Int. J. Mech. Eng. Technol. Appl.*, vol. 3, no. 1, p. 55, Jan. 2022, DOI: 10.21776/MECHTA.2022.003.01.8
[17] S. Wang, M. Gu, S. Yin, Z. Zhou, L. Ma, and F. Qi, "*In-situ* measurement of CO2 column density and flame temperature of single biomass particle combustion by laser absorption spectroscopy," *Chin. J. Chem. Phys.*, vol. 37, no. 6, pp. 745–753, Dec. 2024, DOI: 10.1063/1674-0068/cjcp2408105
[18] Y. Bai *et al.*, "Combustion properties and pollutant analysis of coal-blended bio-heavy oil fuel," *RSC Adv.*, vol. 14, no. 7, pp. 4362–4368, 2024, DOI: 10.1039/D3RA08748D
[19] Y. Jia *et al.*, "Gas-carrying enhances the combustion temperature of the biomass particles," *Energy*, vol. 239, p. 121956, Jan. 2022, DOI: 10.1016/j.energy.2021.121956
[20] N. Čajová Kantová, S. Sładek, J. Jandačka, A. Čaja, and R. Nosek, "Simulation of Biomass Combustion with Modified Flue Gas Tract," *Appl. Sci.*, vol. 11, no. 3, p. 1278, Jan. 2021, DOI: 10.3390/app11031278
[21] M. L. Holtmeyer, G. Li, B. M. Kumfer, S. Li, and R. L. Axelbaum, "The Impact of Biomass Cofiring on Volatile Flame Length," *Energy Fuels*, vol. 27, no. 12, pp. 7762–7771, Dec. 2013, DOI: 10.1021/ef4013505
[22] I. V. Ion, F. Popescu, R. Mahu, and E. Rusu, "A Numerical Model of Biomass Combustion Physical and Chemical Processes," *Energies*, vol. 14, no. 7, p. 1978, Apr. 2021, DOI: 10.3390/en14071978
[23] F. Neves, A. A. Soares, and A. Rouboa, "A Comparison of Different Biomass Combustion Mechanisms in the Transient State," *Energies*, vol. 17, no. 9, p. 2092, Apr. 2024, DOI: 10.3390/en17092092
[24] P. J. Smith and T. H. Fletcher, "A Study of Two Chemical Reaction Models in Turbulent Coal Combustion," *Combust. Sci. Technol.*, vol. 58, no. 1–3, pp. 59–76, Mar. 1988, DOI: 10.1080/00102208808923956
[25] B. F. Magnussen and B. H. Hjertager, "On mathematical modeling of turbulent combustion with special emphasis on soot formation and combustion," *Symp. Int. Combust.*, vol. 16, no. 1, pp. 719–729, Jan. 1977, DOI: 10.1016/S0082-0784(77)80366-4
[26] M. R. Kaiway, Joni, A. Giai, S. P. Siregar, E. Tambing, and O. Pius, "Uncertainty-Quantified Grid-Convergence Analysis of RANS Turbulence Models for 2-D Incompressible Backward-Facing Step Flow in OpenFOAM," *Adv. Sustain. Sci. Eng. Technol.*, vol. 8, no. 1, p. 0260106, Dec. 2025, DOI: 10.26877/asset.v8i1.2390
[27] Ansys, *Ansys Fluent*. [Online]. Available: https://www.ansys.com/
[28] N. Adi Sasongko, N. Gunadi Putra, and M. L. Donna Wardani, "Review of types of biomass as a fuel-combustion feedstock and their characteristics," *Adv. Food Sci. Sustain. Agric. Agroindustrial Eng.*, vol. 6, no. 2, pp. 170–184, Jun. 2023, DOI: 10.21776/ub.afssaae.2023.006.02.8
[29] N. P. Pérez *et al.*, "Unlocking the potential of sugarcane bagasse: a comprehensive analysis for advanced energy conversion," *Bioresour. Bioprocess.*, vol. 12, no. 1, p. 60, Jun. 2025, DOI: 10.1186/s40643-025-00878-5
[30] P. R. S. Oliveira *et al.*, "From waste to watts: Investigating teak biomass waste for bioenergy," *BioResources*, vol. 19, no. 2, pp. 2883–2900, Mar. 2024, DOI: 10.15376/biores.19.2.2883-2900

[31] F. G. Roper, C. Smith, and A. C. Cunningham, “The prediction of laminar jet diffusion flame sizes: Part II. Experimental verification,” *Combust. Flame*, vol. 29, pp. 227–234, Jan. 1977, DOI: 10.1016/0010-2180(77)90113-4

[32] Y. M. Sung *et al.*, “Influence of pulverized coal properties on heat release region in turbulent jet pulverized coal flames,” *Exp. Therm. Fluid Sci.*, vol. 35, no. 4, pp. 694–699, May 2011, DOI: 10.1016/j.expthermflusci.2011.01.003

[33] C. Diblasi, “Modeling chemical and physical processes of wood and biomass pyrolysis,” *Prog. Energy Combust. Sci.*, vol. 34, no. 1, pp. 47–90, Feb. 2008, DOI: 10.1016/j.pecs.2006.12.001

[34] D. Duong, G. Lantos, D. Tillman, D. Kawecki, and A. Coleman, “Biomass Co-firing and its effect on the combustion process,” in *Proceedings of the 35th International Technical Conference on Clean Coal & Fuel Systems*, Clearwater, FL, USA, Jun. 2010, p. 421. [Online]. Available: https://www.proceedings.com/content/008/008954webtoc.pdf

[35] M. A. Delichatsios, “Transition from momentum to buoyancy-controlled turbulent jet diffusion flames and flame height relationships,” *Combust. Flame*, vol. 92, no. 4, pp. 349–364, Mar. 1993, DOI: 10.1016/0010-2180(93)90148-V